BBA - Molecular Basis of Disease 1864 (2018) 11–23

Contents lists available at ScienceDirect

BBA - Molecular Basis of Disease

journal homepage: www.elsevier.com/locate/bbadis

Endogenous osteopontin induces myocardial CCL5 and MMP-2 activation that contributes to inflammation and cardiac remodeling in a mouse model of chronic Chagas heart disease

Eugenia Pérez Caballero[a], Miguel H. Santamaría[a], Ricardo S. Corral[b,*]

[a] Laboratorio de Biología Experimental, Centro de Estudios Metabólicos, Santander, Spain
[b] Servicio de Parasitología-Chagas, Hospital de Niños "Dr. Ricardo Gutiérrez", Buenos Aires, Argentina

ARTICLE INFO

Keywords:
Trypanosoma cruzi
Chagas cardiomyopathy
Inflammation
Cardiac remodeling
Osteopontin

ABSTRACT

Cardiac dysfunction with progressive inflammation and fibrosis is a hallmark of Chagas disease caused by persistent *Trypanosoma cruzi* infection. Osteopontin (OPN) is a pro-inflammatory cytokine that orchestrates mechanisms controlling cell recruitment and cardiac architecture. Our main goal was to study the role of endogenous OPN as a modulator of myocardial CCL5 chemokine and MMP-2 metalloproteinase, and its pathological impact in a murine model of Chagas heart disease. Wild-type (WT) and OPN-deficient (*spp1* −/−) mice were parasite-infected (Brazil strain) for 100 days. Both groups developed chronic myocarditis with similar parasite burden and survival rates. However, *spp1* −/− infection showed lower heart-to-body ratio ($P < 0.01$) as well as reduced inflammatory pathology ($P < 0.05$), CCL5 expression ($P < 0.05$), myocyte size ($P < 0.05$) and fibrosis ($P < 0.01$) in cardiac tissues. Intense OPN labeling was observed in inflammatory cells recruited to infected heart ($P < 0.05$). Plasma concentration of MMP-2 was higher ($P < 0.05$) in infected WT than in *spp1* −/− mice. Coincidently, specific immunostaining revealed increased gelatinase expression ($P < 0.01$) and activity ($P < 0.05$) in the inflamed hearts from *T. cruzi* WT mice, but not in their *spp1* −/− littermates. CCL5 and MMP-2 induction occurred preferentially ($P < 0.01$) in WT heart-invading $CD8^+$ T cells and was mediated *via* phospho-JNK MAPK signaling. Heart levels of OPN, CCL5 and MMP-2 correlated ($P < 0.01$) with collagen accumulation in the infected WT group only. Endogenous OPN emerges as a key player in the pathogenesis of chronic Chagas heart disease, through the upregulation of myocardial CCL5/MMP-2 expression and activities resulting in pro-inflammatory and pro-hypertrophic events, cardiac remodeling and interstitial fibrosis.

1. Introduction

Chronic cardiomyopathy is the most frequent and severe manifestation of Chagas disease, triggered by infection with the protozoan parasite *Trypanosoma cruzi*. It affects approximately one-third of *T. cruzi*-infected patients, typically years or decades after the initial exposure [1]. Multiple mechanisms have been suggested to explain the pathogenesis of parasite-elicited cardiomyopathy, including pathogen persistence, exacerbated inflammatory response, autoimmunity, microvascular disorders and/or neurogenic disturbances [2]. This complex process still remains incompletely understood, but it is now clear that prolonged inflammation due to incessant cardiac parasitism provokes serious damage to the conduction system and myocardium [3,4]. A selective $CD8^+$ T cell trafficking towards the target organ is driven by a mosaic of local chemoattractant agents including adhesion molecules, extracellular matrix components, and pro-inflammatory cytokines and chemokines, particularly CCL2, CCL3, CCL5, CXCL9 and CXCL10 [5]. Focal myocarditis becomes more intense as the disease progresses to severe clinical stages. In advanced cases, the loss of cardiomyocytes and their substitution by fibrotic tissue lead to disruption of muscle fibers and malfunctioning of the electrophysiologic sincitia. Cardiovascular alterations predispose the infected patient to heart failure and ventricular arrhythmias, with increased risk of premature death [6].

Among other cardiopathogenic factors, *T. cruzi* infection induces the production of several inflammatory enzymes, including matrix metalloproteinases (MMPs). This protein superfamily comprises a panel of zinc-dependent endopeptidases that are classified into families according to their substrate specificity [7]. The expression and activities

Abbreviations: OPN, osteopontin; CCL5, chemokine C-C ligand 5; MMP-2, matrix metalloproteinase-2; WT, wild-type; *Spp1* −/−, lacking the *spp1* gene coding for osteopontin; dpi, days post infection; SD, standard deviation; ANOVA, one-way analysis of variance; MAPK, mitogen-activated protein kinase; JNK, jun NH_2-terminal kinase; AP-1, activator protein 1; TRE, TPA-responsive element

* Corresponding author at: Servicio de Parasitología-Chagas, Hospital de Niños "Dr. Ricardo Gutiérrez", Gallo 1330, CP1425 Ciudad Autónoma de Buenos Aires, Argentina.
E-mail address: ricardocorral@conicet.gov.ar (R.S. Corral).

http://dx.doi.org/10.1016/j.bbadis.2017.10.006
Received 19 June 2017; Received in revised form 21 September 2017; Accepted 3 October 2017
Available online 04 October 2017

of MMPs are strictly controlled under normal circumstances, but often become activated in the development of diverse pathologies, such as neoplasia, arthritis, and neurodegenerative and cardiovascular disorders [8,9]. In addition, overexpression of MMPs has been associated with tissue remodeling during infections with protozoan parasites [10]. In experimental *T. cruzi* infection, increased levels of the gelatinases MMP-2 and MMP-9 have been suggested to contribute to acute myocarditis by favoring leukocyte infiltration and modulating immunity [11,12]. Moreover, enhanced MMP-2 and MMP-9 expression has been linked to the cardiac clinical form in chronic Chagas patients. Both enzymes have been postulated as potentially useful biomarkers of the progression to severe *T. cruzi* cardiomyopathy, as well as promising therapeutic targets [13–15]. Regarding the control of gelatinase levels, the cytokine and cell attachment phosphoprotein osteopontin (OPN) has been implicated in the upregulation of MMP-2 expression and activity in tumor cells [16], and also in orchestrating inflammation against *T. cruzi* [17]. In the present study, we investigated the role of endogenous OPN as a modulator of myocardial CCL5 and MMP-2, as well as its pathological impact in a murine model of chronic Chagas heart disease.

2. Material and methods

2.1. Ethics statement

This study was carried out in strict accordance with the recommendations of Spanish Legislation and the European Union Directive (2010/63/EU) for the protection of animals used for scientific purposes. All mice were maintained under pathogen-free conditions in the animal facility at the Centro de Estudios Metabólicos (Santander, Spain). The animal protocol was approved by the Comité de Ética en la Investigación de la Universidad de Oviedo (Asturias, Spain). The individual room temperatures were kept between 18 and 22 °C with food and water *ad libitum*. Care of the mice was overseen by a laboratory animal veterinarian, in compliance with European codes of practice. Mice were euthanized in a CO_2 chamber, and all efforts were made to minimize suffering.

2.2. Mice and infection

OPN-deficient (*spp1* −/−) and wild-type (WT) mice breeded into a C57BL/6 genetic background were purchased from The Jackson Laboratory (Bar Harbor, ME, USA). Ten adult (six- to eight-week-old) male mice from each genotype were infected by intraperitoneal injection of 10^3 trypomastigotes of *T. cruzi* Brazil strain [18] (routinely maintained by serial subinoculation in C3HeJ mice at three-week intervals) in 0.1 ml blood. Age- and sex-matched uninfected WT and OPN deficient mice (ten mice per group) were used as controls. For each group, body weight and mortality rate were recorded daily. Blood specimens were collected and mice were sacrificed at 100 days post infection (dpi). The hearts were excised, weighed and processed for parasite, chemokine and enzyme detection, histopathological examination, and immunohistochemical studies.

2.3. Cardiac parasitism

DNA from the hearts of mice was isolated with High Pure PCR Template Preparation Kit (Roche Applied Science, Indianapolis, IN, USA), according to the manufacturer's instructions. For parasite detection, we used the quantitative PCR assay described by Caldas et al. [19]. The reactions were performed with 100 ng of genomic DNA. The results were based on a standard curve constructed with DNA (0.01–100 pg) from culture specimens of *T. cruzi* trypomastigotes. The standards for the quantitative PCR reactions were generated from tissue homogenate of heart from naïve mice, to which 2×10^4 trypomastigotes were added per mg of tissue. DNA (from tissues spiked with parasites) was extracted and serially diluted with DNA obtained from parasite-free myocardium. The ten-fold diluted prepared standards contained DNA from 5×10^2 to 5×10^{-2} parasite equivalents (estimated DNA content of *T. cruzi*: 0.22 pg/parasite, varying from 0.12 to 0.33) per 100 ng of total DNA. A standard curve was generated from these standards to determine the DNA pathogen load in the infected hearts.

2.4. Histopathological and immunohistochemical analyses of heart

Cardiac tissues from mice were cut in pieces and placed in 10% neutral buffered formalin for at least 4 h at room temperature followed by overnight incubation in 70% ethanol. Samples were embedded in paraffin and 5-μm tissue sections were cut onto coated slides and stained with hematoxylin-eosin or using the Masson's trichrome staining. Myocardial sections were examined for evaluation of the inflammatory and degenerative processes. This analysis was performed in at least twenty areas in each heart section, in three sections from each animal, at 400× magnification (50 microscopic fields examined). Morphometric analysis of cardiomyocytes and quantification of leukocyte accumulation were accomplished by standard procedures [20,21]. Analysis and quantification of interstitial fibrotic injury was evaluated as fractional area of collagen content in % of total myocardial tissue with a digital image software (ImageJ-NIH, Bethesda, MD, USA). For the determination of fibrosis, at least 60 fields per group were assessed.

For immunohistochemical studies, the slides were deparaffinized and rehydrated using routine techniques. Then, tissue sections were incubated in citrate buffer (10 mM sodium citrate, 0.05% Tween-20, pH 6.0) for 30 min at 95 °C for antigen retrieval, followed by treatment with 0.3% hydrogen peroxide and blocking with 10% normal goat or rabbit serum. Specimens were finally analyzed using goat polyclonal antibody to OPN (1: 20; R & D Systems, Minneapolis, MN, USA) and biotinylated rabbit antiserum to goat IgG (Vector Laboratories, Burlingame, CA, USA), or rabbit polyclonal antibody to MMP-2 (1:1000; Torrey Pines Biolabs, San Diego, CA, USA) and biotinylated swine antiserum to rabbit immunoglobulin (Dako, Glostrup, Denmark), following a procedure previously described [22]. Mouse β-actin detection by a monoclonal antibody (AC-15, 1:50, Sigma-Aldrich, St. Louis, MO, USA) was used for normalization of mean staining intensities with OPN (or MMP-2)/β-actin ratio.

2.5. Isolation of $CD4^+$ and $CD8^+$ T cells from the leukocyte infiltrate

Hearts from twenty *T. cruzi*-infected mice (100 dpi) were enzymatically digested at 37 °C with 200 FALGPA U/ml collagenase type IV from *Clostridium histolyticum* and 200 FALGPA U/ml hyaluronidase type IV-S (Sigma-Aldrich) to isolate inflammatory cells. The mononuclear cell fraction was separated by centrifugation on Histopaque 1083 (Sigma-Aldrich) [23] and washed twice with PBS plus 5% heat inactivated fetal calf serum (FCS). Aliquots of these cells were suspended in RPMI 1640 culture medium supplemented with 10% FCS and 1.5 mM L-glutamine. All the media and reagents were endotoxin-free. Cells were seeded by triplicate in 24-well plates and stimulated with *T. cruzi* trypomastigote lysate (10 μg/ml) [17] for 24 h at 37 °C. Infiltrating $CD4^+$ and $CD8^+$ T cells were then isolated using immunomagnetic negative selection (EasySep™ TM Mouse $CD4^+$ and $CD8^+$ Isolation Kits, StemCell Technologies, Grenoble, France) following the manufacturer's instructions. Each subpopulation (5×10^5 cells/well) was cultured for another three days in the presence of anti-mouse CD3 antibody (clone: 145-2C11 from BD Biosciences-Pharmingen, San José, CA, USA) conjugated nanoparticles (40 nM, Explora Biotech, Rome, Italy) to selectively activate *T. cruzi*-experienced T cells [24].

2.6. Real-time PCR

Quantitative real-time RT-PCR analysis was performed using the High Capacity cDNA Archive Kit (Applied Biosystems, Foster City, CA, USA), and amplification of murine genes (*Ccl5*, *Ccl3*, *Cxcl9*, *Cxcl10* and ribosomal 18S) was performed in triplicate with the use of TaqMan MGB probes and the TaqMan Universal PCR Master Mix (Thermo Fisher Scientifics, Waltham, MA, USA) on an ABI Prism 7900 HT instrument (Applied Biosystems), as reported previously [25,26]. Quantification of gene expression was calculated using the comparative threshold cycle method, normalized to the ribosomal 18S control and efficiency of the RT reaction (relative quantity, $2^{-\Delta\Delta CT}$).

2.7. Hydroxyproline quantification

Fragments of 100 mg of myocardium were removed for hydroxyproline determination, as an indirect measure of fibrotic deposition of collagen [27]. Briefly, tissues were homogenized in saline 0.9%, frozen at − 70 °C and lyophilized. The assay was performed with 20 mg of dry tissue, which was subjected to alkaline hydrolysis in 300 μl H_2O plus 75 μl 10 M NaOH at 120 °C for 20 min. An aliquot of 50 μl of the hydrolyzed tissue was added to 450 μl of Chloramine T oxidizing reagent (56 mM Chloramine T, 10% *n*-propanol in citrate buffer) and allowed to react for 20 min. A hydroxyproline standard curve was prepared likewise. Color was developed by addition of 500 μl of 1 M *p*-dimethyl-aminobenzaldehyde diluted in n-propanol/perchloric acid 2:1 v/v. Optical density was read at 550 nm.

2.8. Gelatin zymography

The catalytic activity of MMP-2 was examined by gelatin zymography of cardiac tissue homogenate, as described elsewhere [11]. In brief, 30 μg of protein from heart homogenate were electrophoresed through a 7.5% polyacrylamide gel copolymerized with 1 mg/ml gelatin (type A from porcine skin; Sigma-Aldrich). The gels were then washed twice with 2.5% Triton X-100 and incubated for 24 h at 37 °C in activation buffer (50 mM Tris-HCl buffer, pH 7.4, containing 10 mM $CaCl_2$ and 1 μM $ZnCl_2$). After incubation, the gels were stained with 0.05% Coomassie brilliant blue, and destained with 10% acetic acid and 30% methanol in H_2O. Gelatine degradation was visualized as transparent bands against the dark background. To confirm the specificity of the metalloproteinase activity detected, and to standardize results from different zymograms, recombinant mouse MMP-2 (BioLegend, San Diego, CA, USA) was used as a positive internal control. For correlation analysis, MMP-2 activity as detected by gelatin zymography was further measured by transmission densitometry (G-700 Densitometer; Bio-Rad, Hercules, CA, USA) and results were expressed as fold change over uninfected control samples.

2.9. Assessment of soluble chemokine and metalloproteinase levels

Commercial ELISA kits were used to evaluate levels of murine CCL3, CCL5, CXCL9, CXCL10, MMP-2 (R & D Systems), and MMP-10 (MyBioSource, San Diego, CA, USA) in cell supernatants and plasma samples, according to the manufacturers' instructions. The supplied standards were used to generate the corresponding standard curves. The assay sensitivity for CCL3, CCL5, CXCL9, CXCL10, MMP-2 and MMP-10 was 1.5 pg/ml, 2.0 pg/ml, 7.8 pg/ml, 4.2 pg/ml, 0.082 ng/ml and 2.35 pg/ml, respectively.

2.10. Western blotting

Heart samples were homogenated by a modified RIPA buffer containing 1% Nonidet P-40, 0.25% sodium deoxycholate, 0.1% SDS, 1 mM EDTA, and a protease/phosphatase inhibitor cocktail (Calbiochem, EMD Millipore, Danvers, MA, USA). After centrifugation at 15,000 x g for 20 min at 4 °C, the supernatants of cell lysates containing 30 μg protein each were subjected to 10% SDS-PAGE and transferred to a nitrocellulose membrane (EMD Millipore). The filters were probed with mitogen-activated protein kinase (MAPK) antibodies specific for total p38 and phosphorylated p38 (Cell Signaling Technology, Danvers, MA, USA), or total Jun NH_2-terminal kinase (JNK) and phosphorylated JNK (Cell Signaling), used at 1:1000 dilution. A HRP-conjugated appropriate secondary antibody was dispensed to detect immunoreactive bands using an ECL system (GE Healthcare, Pittsburgh, PA, USA).

Band intensity was analyzed using NIH Image J software.

2.11. c-Jun DNA-binding activity

Nuclear extracts (15 μg) were prepared from both uninfected and infected heart tissues using the Qproteome Nuclear Protein Kit (Qiagen, Germantown, MD, USA) and applied to an activator protein 1 (AP-1)/c-jun transcription factor assay kit (TransAM®, Active Motif, Carlsbad, CA, USA) according to the manufacturer's recommendations [28]. Phosphorylated c-jun present in nuclear protein extract binds specifically to an oligonucleotide containing a TPA-responsive element (TRE) with the consensus binding site 5′-TGAGTCA-3′ immobilized on the microplate. In some experiments, a competitor oligonucleotide (original TRE or mutant) was added to confirm specific reactivity. The c-jun antibody recognizes an epitope on the protein that is accessible upon DNA binding. Addition of a secondary HRP-conjugated antibody and the corresponding substrate provided a sensitive colorimetric readout quantified by spectrophotometry.

2.12. Flow cytometry

Flow analysis was used to ensure adequate enrichment of isolated cell subsets. The cells were first stained extracellularly with labeled rat anti-mouse CD4-PerCP-Cy 5.5 (RM4-5, 1:200 dilution) and CD8a-Alexa Fluor 647 (53-6.7, 1:200) antibodies (BD Biosciences-Pharmingen), and then fixed and permeabilized with BD Cytofix/Cytoperm solution (BD Biosciences-Pharmingen). Specific gating strategies were used to select the lymphocyte population. The purity of enriched cell preparations was: $CD4^+$, 95.6 ± 1.2 (mean% ± SD); $CD8^+$, 94.7 ± 1.3. Each subset was gated on the 7-amino actinomycin D negative ($7\text{-}AAD^-$), live cell population. Mean cell viability was: $CD4^+$, 81%; $CD8^+$, 89% as judged by this test. The cells were next separately stained intracellularly with mouse PE-conjugated anti-murine CCL5 (2E9/CCL5, 1:200, BioLegend), Alexa Fluor 488-conjugated rabbit anti-mouse MMP-2 (NB200-193AF488, 1:250, Novus Biologicals, Littleton, CO, USA), or isotype control immunoglobulins. Antibodies were added to the cell suspension at a final volume of 100 μl and incubated in the darkness at 2–8 °C for 30 min. Samples (at least 5×10^5 cells) were acquired on a FACSCalibur (BD Biosciences) and data were analyzed using BD CellQuest Pro software (BD Biosciences).

2.13. Effect of JNK inhibitor on inflammatory response

$CD8^+$ T cells isolated by immunomagnetic selection from inflammatory infiltrates present in myocardium from *T. cruzi*-infected WT and *spp1* −/− mice were stimulated with trypomastigote lysate for 24 h. Then, the cells were split into 96-well plates at a density of 1×10^6 leukocytes/well. Activation was achieved by 72-h incubation with anti-CD3 conjugated nanoparticles in the presence of 10 μM SP600125 JNK inhibitor (Tocris Bioscience, Bristol, UK) or DMSO vehicle. This step was followed by cell surface marker labeling, fixation and impermeabilization, before intracellular staining with antibodies to CCL5 and MMP-2. Percentages of chemokine- and metalloproteinase-synthesizing cells were measured by FACSCalibur flow cytometer and analyzed by CellQuest Pro software.

2.14. Statistical analysis

Statistical analysis was performed by using GraphPad Prism (San Diego) 5.0 software. Arithmetic means and standard deviations (SD), derived from at least three different observations for each sample analyzed in independent experiments, were calculated. Significant differences among multiple groups were made by using the one-way analysis of variance (ANOVA) test followed by Tukey's test. Wilcoxon signed rank test was conducted for comparisons between two groups. Correlation analyses were done using Pearson's correlation coefficient. In all cases, values of $P < 0.05$ were considered statistically significant.

3. Results

3.1. OPN deficiency ameliorates inflammatory cardiomyopathy, heart fibrosis and CCL5 induction in mice chronically infected with T. cruzi

Mice bred on a C57BL/6 background, when infected with the Brazil strain of *T. cruzi*, are known to overcome the acute phase of Chagas disease and gradually develop a dilated cardiomyopathy by 100 dpi [29]. At that time of infection, examination of the hearts of *T. cruzi*-infected mice revealed significantly ($P < 0.05$) increased OPN expression in cardiac tissue (Fig. 1A). We observed immunostaining for OPN mostly localized in leukocytes infiltrating the inflammatory lesions of the myocardium. On the other hand, heart sections from uninfected mice displayed no enhanced levels of the phosphoprotein. OPN antibody showed no IHC reactivity in different *spp1* −/− tissues (heart, liver, spleen, skeletal muscle, lymph nodes), either infected or uninfected (data not shown). The role of OPN in the development of *T. cruzi*-dependent cardiomyopathy was then analyzed in mice with or without genetic double deficiency in OPN chronically infected with the parasite. In our series, no differences in parasite burden in myocardium and survival rate were found between WT and *spp1* −/− mice at 100 dpi. Nevertheless, the heart-to-body weight ratio was significantly ($P < 0.01$) lower in the group devoid of endogenous OPN (Table 1). In the infected WT animals, the histopathological examination revealed mild cardiomyocyte hypertrophy (Fig. 1B). We found a significant ($P < 0.05$) increase in the cross-sectional area of cardiac muscle cells, supporting that the high heart-to-body weight ratio resulted -at least in part- from an enlargement of the myocytes themselves, as opposed to edema which might augment the organ weight. The chronic sequelae present by day 100 included marked thinning, focal inflammation and fibrosis in the right and left ventricular walls of the heart, with destruction of cardiac myofibers. *T. cruzi*-infected WT animals exhibited widespread leukocyte infiltration in heart tissue, accompanied by diffuse interstitial fibrosis. However, in infected mice with genetic ablation of *spp1* there was a significant ($P < 0.05$) reduction of the intensity of long-term inflammatory pathology and myocyte size in myocardium (Fig. 1B). In parallel, the amount of interstitial fibrosis in the organ was significantly ($P < 0.01$) less as demonstrated by Masson's trichrome staining and hydroxyproline quantification, representative of tissue collagen deposition (Fig. 1B and C). Independently of their endogenous OPN availability, uninfected C57BL/6 mice showed neither areas of deposition of myocardial collagen nor remarkable increase of hydroxyproline content (Fig. 1B and C).

Local production of the pro-inflammatory chemokines CCL3, CCL5, CXCL9 and CXCL10 at the target site of persistent infection with *T. cruzi* (100 dpi) was also studied. Elevated mRNA (Fig. 2A) and protein (Fig. 2B) levels of the four chemoattractants were detected in cardiac muscle from the infected WT group in comparison to uninfected counterparts ($P < 0.05$). Conversely, parasite-infected *spp1* −/− mice displayed downregulated generation of CCL5 transcript and protein compared to that recorded for infected WT littermates ($P < 0.05$), whereas augmented CCL3, CXCL9 and CXCL10 expression remained unaltered. Altogether, these findings suggest that CCL5 induction, pathological inflammation and collagen accumulation in the heart during experimental chronic *T. cruzi* infection are at least partially modulated by endogenous OPN.

3.2. OPN-deficient mice display reduced expression and activity of myocardial MMP-2 during the chronic phase of experimental Chagas disease

Excessive activation of MMP-2 and MMP-10 has been implicated in adverse cardiac remodeling upon chronic cardiomyopathy [30,31]. Therefore, we analyzed *T. cruzi*-induced production of both enzymes in our infection model. First, we detected increased concentrations of MMP-2 and MMP-10 in the blood of chronically infected WT mice displaying myocardial abnormalities compared to the uninfected group. Notably, MMP-2, but not MMP-10, plasma levels in *T. cruzi*-infected *spp1* −/− mice were found to be significantly ($P < 0.05$) lower than those recorded in their WT littermates infected with the parasite (Fig. 3A). We further assessed myocardial MMP-2 protein expression by immunohistochemistry. Specific staining revealed the presence of the enzyme in heart muscle from WT mice on day 100 of infection, mainly associated with areas of leukocyte infiltration. Such immunoreactivity was significantly ($P < 0.01$) higher than that visualized in specimens from OPN-deficient mice chronically infected with *T. cruzi* (100 dpi) or uninfected animals (Fig. 3B). To investigate whether the upregulated expression of myocardial MMP-2 was linked to augmented gelatinase activity, gelatin zymography was carried out on cardiac tissue extracts from mice on day 100 after infection and uninfected controls. We verified that the hearts from WT mice with chronic Chagas myocarditis displayed much higher ($P < 0.05$) gelatinolytic activity of the active form of MMP-2 (62 kDa) than that observed for the infected *spp1* −/− group or pathogen-free mice (Fig. 3C). These findings show that endogenous OPN has a remarkable participation in the induction of cardiac MMP-2 expression and activity upon prolonged *in vivo* infection with *T. cruzi*.

3.3. Endogenous OPN modulates the phospho-JNK MAPK signaling pathway in the heart from chronically infected mice

In an attempt to clarify the molecular mechanisms underpinning OPN-mediated cardiopathogenesis during the chronic stage of *T. cruzi* infection, we investigated the contribution of MAPK cascade in myocardium from infected mice. Immunoblot analysis revealed that parasite infection significantly ($P < 0.05$) activated the intracellular JNK signaling pathway in cardiac cells from WT but not *spp1* −/− animals, without changes in their total protein content (Fig. 4A). Differentially, we detected a very weak induction of myocardial p38 phosphorylation for both infected groups. Furthermore, augmented expression of phospho-JNK promoted by OPN was associated with enhanced AP-1 DNA-binding activity. We found that OPN generated upon prolonged *T. cruzi* infection of WT mice induced a 5.5-fold increase ($P < 0.01$) of c-jun recognition of the 5′-TGAGTCA-3′ motif over values obtained from infected *spp1* −/− mice. Specificity of the assay was confirmed by competitive binding studies, in which oligonucleotides containing an unmodified consensus (TRE competitor), but not a mutant (mut competitor), c-jun target sequence significantly ($P < 0.05$) attenuated binding to the immobilized probe (Fig. 4B). These results suggest that, in chronic Chagas heart disease, endogenous OPN is implicated in upregulation of the phospho-JNK MAPK signaling route in *T. cruzi*-infected myocardium.

3.4. OPN-induced CCL5 and MMP-2 molecules are mainly produced by $CD8^+$ T cells present in the inflammatory heart infiltrate of chronically infected mice

The ability of endogenous OPN to upregulate myocardial CCL5 and MMP-2 levels in mice chronically infected with *T. cruzi* prompted us to search for the cellular source of these pro-inflammatory mediators.

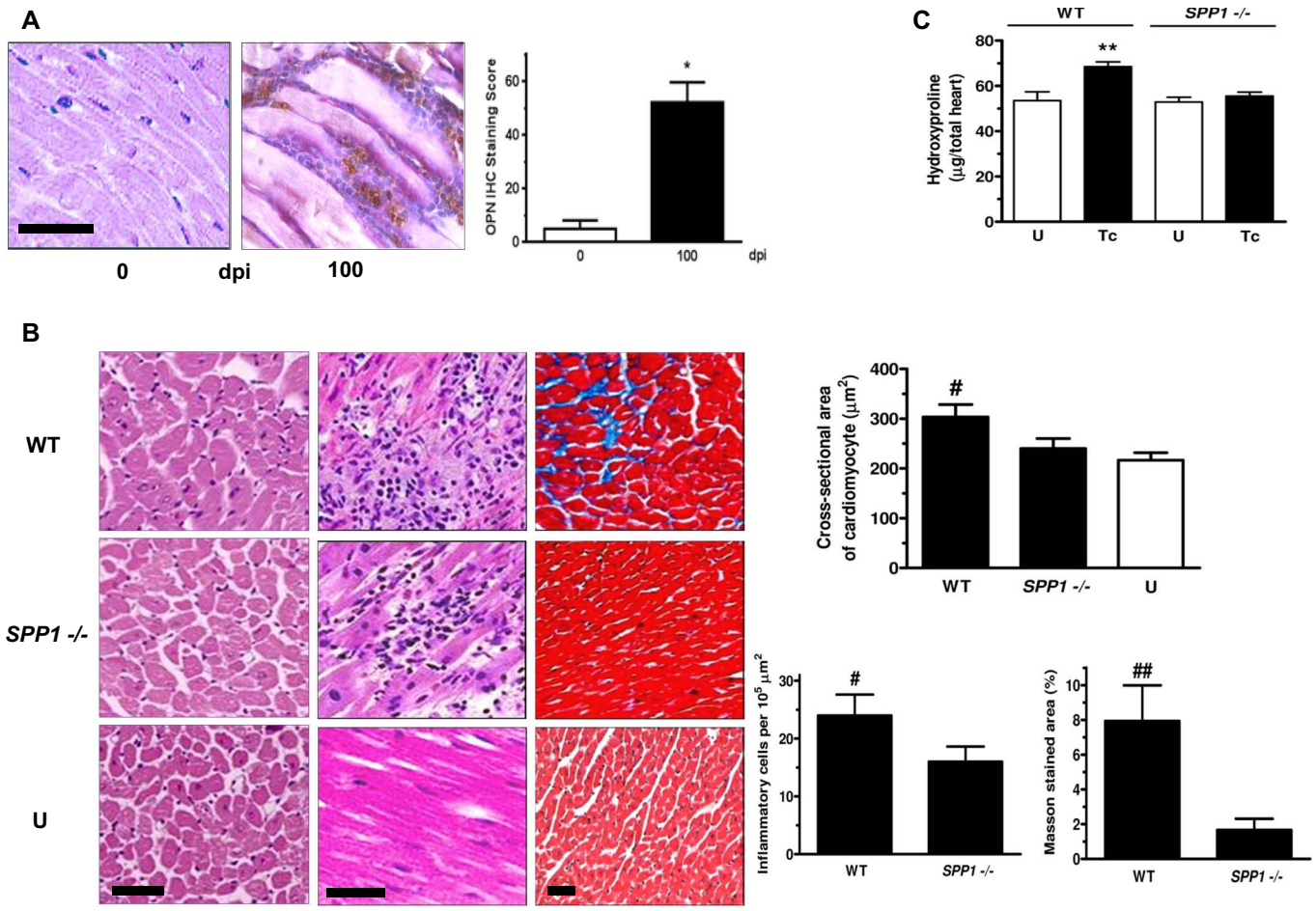

Fig. 1. Myocardial osteopontin (OPN), inflammatory lesions and collagen deposition in mice chronically infected with *T. cruzi*.
Wild-type (WT) and OPN-deficient (*spp1* −/−) C57BL/6 mice were infected with the parasite for 100 days. Uninfected mice (U) were included as a control group. After that period, ten animals from each group were sacrificed and their hearts were collected for histopathological studies.
(A) Immunostaining of cardiac muscle sections was performed using OPN-specific polyclonal antibody. Images show a representative experiment of three performed; scale bar: 100 µm. dpi, days post infection. Quantification was performed by scoring the staining intensities using ImageJ (NIH), as described in 'Material and methods'. Results are means ± SD, $^{*}P < 0.05$. Data are representative of three independent experiments with at least eight mice per group each.
(B) Microphotographs of tissue-sections from each experimental group stained with hematoxylin-eosin (left and central panels) and Masson's trichrome stain (right panels); scale bar: 50 µm. Cardiomyocyte cross-sectional area, infiltrating inflammatory cells and Masson-stained area were measured in infected (black bars) and uninfected (white bars) heart tissue specimens. The measurements were done in three independent experiments. Results from digital image analysis applied for quantification are shown. Data (means ± SD) are derived from at least eight mice per group. $\#P < 0.05$ *versus* uninfected and infected *spp1* −/− mice; $\#\#P < 0.01$ *versus spp1* −/− infection.
(C) Hydroxyproline content in myocardium of uninfected (U) and *T. cruzi*-infected (Tc) animals. Myocardia were excised at 100 dpi. Hydroxyproline content was evaluated by colorimetric assay. Values, expressed as means ± SD from three separate experiments, are representative of at least eight mice per group. $^{**}P < 0.01$ when comparing infected WT mice *versus* the remaining groups.

Table 1
Chronic *Trypanosoma cruzi* infection in wild-type (WT) and osteopontin-deficient (*spp1* −/−) C57BL/6 mice.

Genotype	Heart/body weight ratio (mg/g)	Heart parasitism[a]	Survival (%)
WT	7.3 ± 0.5	197 ± 17	100
spp1 −/−	5.2 ± 0.5**	203 ± 15	100

Ten animals per experimental group were analyzed after 100 days of infection with Brazil strain parasites.
Results are expressed as mean ± SD of three independent experiments.
[a] Number of parasite equivalents per 100 ng DNA.
** $P < 0.01$.

Numerous lines of evidence indicate that a marked influx of $CD4^+$ and $CD8^+$ T cells is responsible for aberrant production of multiple pathogenic factors at cardiac tissue of infected mice [32]. We therefore investigated whether CCL5 and MMP-2 were synthesized by such cell subsets within the mononuclear leukocyte population. All data shown was gated on the 7-AAD negative, live $CD4^+$ and $CD8^+$ T cell compartments (Fig. 5A). Intracellular chemokine and metalloproteinase analysis of infiltrating $CD4^+$ and $CD8^+$ T cells performed *ex vivo* demonstrated that there is an expansion of lymphocytes co-expressing CD8/CCL5 and CD8/MMP-2 in the hearts from infected WT mice (Fig. 5B). In this experimental group, $CD4^+CCL5^+$ and $CD4^+MMP\text{-}2^+$ infiltrating cells were present at lower percentages (median values of 28.9% and 4.1%, respectively, *versus* 66.3% $CD8^+CCL5^+$ and 61.4% $CD8^+MMP\text{-}2^+$) (Fig. 5B and Supplemental Fig. 1). Cells were negative for staining with isotype control antibodies. On the other hand, as shown in Fig. 5B, $CD4^+$ and $CD8^+$ T cells isolated from infected *spp1* −/− myocardium displayed only reduced to negligible levels of CCL5 and MMP-2 expression. Of note, the percentage values of $CD8^+CCL5^+$ and $CD8^+MMP\text{-}2^+$ found in infected WT hearts were significantly greater than those recorded in the *spp1* −/− group ($P < 0.01$ and $P < 0.001$, respectively) (Supplemental Fig. 1). For $CD4^+CCL5^+$ and $CD4^+MMP\text{-}2^+$ infiltrating cells, no significant differences were demonstrated between WT and *spp1* −/− mice. In *T. cruzi*-infected hearts showing OPN overexpression, the $CD8^+$ T cell compartment within the inflammatory infiltrate represents a major source of CCL5 and MMP-2

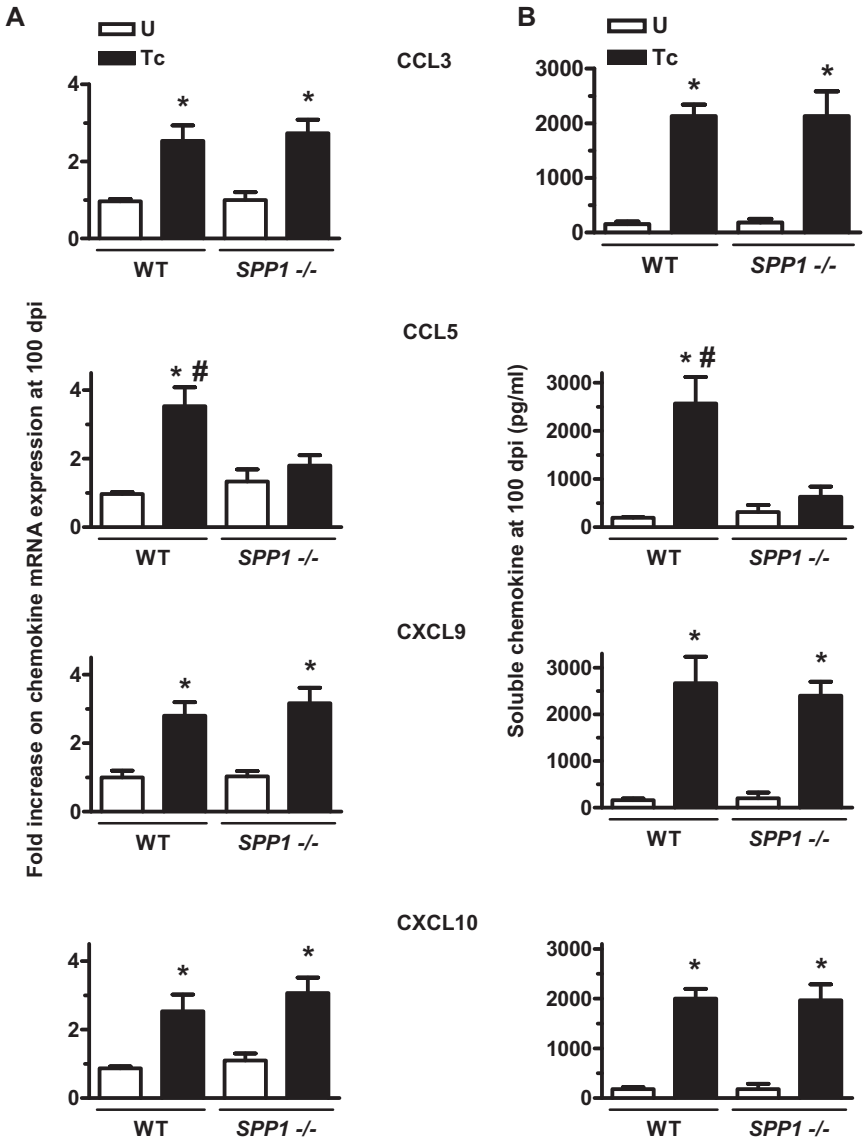

Fig. 2. Pro-inflammatory chemokine expression in the heart during the chronic phase of *T. cruzi* infection (Tc, black bars) in WT and *spp1* −/− mice.
(A) mRNA levels of (C-C motif) ligand 3 (CCL3), CCL5, (C-X-C motif) ligand 9 (CXCL9) and CXCL10. RNA isolated from heart tissue at 100 days post infection (dpi) was used to perform real-time RT-PCR with specific probes, and normalized to ribosomal 18S RNA as described in 'Material and methods'.
(B) Soluble protein concentration of CCL3, CCL5, CXCL9 and CXCL10 as determined by ELISA. Chemokine levels were measured by ELISA using cell supernatants from heart homogenate (100 dpi samples, see 'Material and methods').
Specimens from uninfected mice (U, white bars) were also analyzed. Data are representative of ten mice per group. Values are expressed as means ± SD from three independent infections. *$P < 0.05$ *versus* U group; #$P < 0.05$ *versus* Tc *spp1* −/− mice.

molecules associated with chronic cardiopathogenesis.

3.5. Inhibition of JNK MAPK signaling pathway dampens CCL5 and MMP-2 expression in myocardial $CD8^+$ T cells from T. cruzi-infected mice

Inhibition of the JNK/phospho-c-jun cascade was tested to show its involvement in augmented production of CCL5 and MMP-2 by invading $CD8^+$ T cells selected from infected hearts. FACS analysis demonstrated increased expression levels of both mediators in $CD8^+$ leukocytes constituting the inflammatory infiltrate isolated from the infected WT myocardium. CCL5 and MMP-2 percentage values were markedly ($P < 0.05$) reduced by incubation of cells in the presence of the JNK MAPK-specific inhibitor SP600125 (Fig. 6). $CD8^+$ T cells from infected *spp1* −/− hearts showed low expression of these pro-inflammatory agents and non-significant response to SP600125 treatment. No substantial downregulation was achieved using the p38 MAPK-specific inhibitor SB203580 in WT and *spp1* −/− cell cultures (data not shown). There was no toxic effect of inhibitors on cell viability. These results suggest that, in chronic Chagas heart disease, targeted pharmacological inhibition of phospho-JNK MAPK signaling may reduce myopathy-promoting CCL5 and MMP-2 responses from muscle-infiltrating $CD8^+$ T cells.

3.6. Heart levels of OPN, CCL5 and MMP-2 correlate with the extent of T. cruzi-elicited myocardial fibrosis

Correlations between either cardiac CCL5 concentration or MMP-2 activity and OPN expression at the heart of infected WT mice are displayed in Fig. 7. Both CCL5 and MMP-2 values correlated independently with OPN levels, showing Pearson's coefficients of $r = 0.840$ ($P = 0.002$) and $r = 0.760$ ($P = 0.010$), respectively (Fig. 7A and B). In addition, we estimated correlations between each inflammatory mediator and pathologic structural changes of the infected myocardium. For the correlations between OPN expression, CCL5 level or MMP-2 gelatinase activity, and collagen area fraction in cardiac muscle from infected WT mice, Pearson's coefficients were determined to be $r = 0.930$ ($P = 0.001$), $r = 0.880$ ($P = 0.007$), and $r = 0.900$ ($P = 0.004$), respectively (Fig. 7C–E). Conversely, the correlations between CCL5 concentration or MMP-2 activity and collagen content in the infected *spp1* −/− group were not significant [$r = -0.456$ ($P = 0.185$) and $r = 0.383$ ($P = 0.274$), respectively] (Fig. 7F and G). Collectively, our findings suggest that upregulated production of myocardial OPN, CCL5 and MMP-2 is strongly associated with inflammatory damage and adverse remodeling of the heart during chronic Chagas cardiomyopathy.

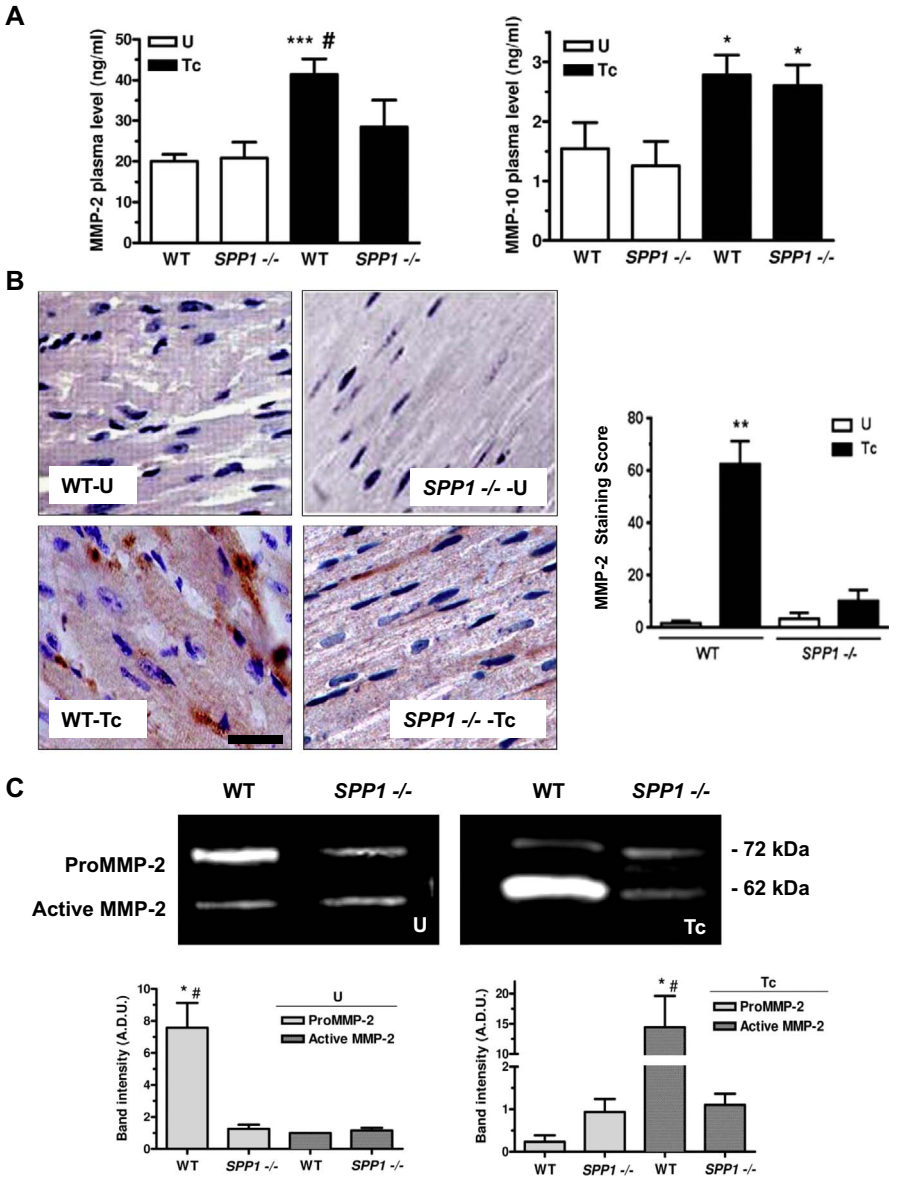

Fig. 3. Circulating levels of matrix metalloproteinases and myocardial gelatinase expression and activity in chronic murine *T. cruzi* infection.

(A) Levels of matrix metalloproteinase (MMP)-2 and MMP-10 in plasma specimens collected from uninfected (U, white bars) and *T. cruzi*-infected (Tc, black bars) C57BL/6 mice. After 100 days of infection, samples obtained from wild-type (WT) and osteopontin-deficient (*spp1* −/−) mice (ten animals from each group were analyzed) were assayed in triplicate by capture ELISA for MMP-2 and MMP-10. Each bar represents the mean values for each group ± SD. The results presented are representative of three independent experiments with similar outcome. $^{*}P < 0.05$ and $^{***}P < 0.001$, compared with U groups; $^{\#}P < 0.05$, compared with Tc *spp1* −/− mice.

(B) MMP-2 expression in heart from *T. cruzi*-infected (Tc, 100 days post infection; black bars) WT and *spp1* −/− mice. Myocardia from uninfected (U, white bars) WT and *spp1* −/− mice were analyzed as well. Panels display representative results of MMP-2-specific immunostaining in cardiac tissues from the different groups and quantitative comparison (mean of three independent determinations ± SD). Data are representative of at least eight mice per group. Original magnification for microphotographs, × 400; scale bar: 20 μm.

(C) Analysis of the influence of endogenous osteopontin on MMP-2 activity. Heart tissues from uninfected (U) and *T. cruzi*-infected (Tc, 100 days) WT and *spp1* −/− mice were subjected to gelatin zymography to detect the enzymatic activity of MMP-2. Representative zymography gel images of MMP-2 (glycosylated proMMP-2 form corresponding to ~72 kDa and active form corresponding to ~62 kDa) are shown. Quantification of bands was accomplished by densitometry. The results presented are representative of three independent experiments performed with ten mice per group. A.D.U., arbitrary densitometric units. $^{*}P < 0.05$ *versus* active MMP-2; $^{\#}P < 0.05$ *versus* proMMP-2 in U- and Tc- *spp1* −/− groups.

4. Discussion

MMPs have been largely related to development of myocarditis caused by prolonged infections of diverse etiology [33–35]. In particular, increased MMP-2 activity has been implicated in the transition from hypertrophy to heart failure, whereas MMP-9 has been linked to chronic inflammatory cardiomyopathy *via* activation of endothelial and myocyte apoptotic pathways rather than promoting fibrosis [36–38]. With regard to human chronic Chagas heart disease, MMP-2 and MMP-9 have been characterized as useful biomarkers for detecting the advent and progression of cardiomyopathy, even with predictive potential on mortality [13,15,39–42]. Of note, the MMP-2/MMP-9 ratio was found to reach significantly higher values in *T. cruzi*-infected patients displaying ECG abnormalities [43]. Moreover, MMP-2 overexpression and enhanced activity appear to rise progressively with increasing complexity of left ventricular dysfunction and cardiac hypertrophy in individuals with advanced-stage infection by this parasite [14,15].

In this study we showed that the expression and activity of MMP-2 are upregulated in cardiac tissue during the chronic phase of *T. cruzi* infection. Such increase is detected in association with abundant inflammatory cells infiltrating the myocardium. More important, we found that the pleiotropic cytokine OPN plays a critical role in the selective induction of myocardial MMP-2 expression and enzymatic activity that leads to exacerbated inflammation and cardiac remodeling in C57BL/6 mice infected for 100 days with Brazil parasite strain. This is a well-defined and reliable animal model for human Chagas heart involvement, for which extensive histopathological, electrocardiographical and imaging data is available [18,44–46]. The ability of OPN to stimulate MMP-2 production and catalytic actions has already been demonstrated in hepatocellular carcinoma cell lines [16]. In a previous report, we have verified that OPN is involved in the modulation of the inflammatory response against *T. cruzi* [17]. Our current data reveal that *T. cruzi*-triggered overexpression of this phosphoprotein by heart-invading mononuclear cells may further contribute to the pathogenesis of Chagas myocarditis favoring MMP-2-dependent leukocyte recruitment and chronic alterations in cardiac structure and function.

OPN is a multi-faced cytokine synthesized by a variety of cell types including fibroblasts, myocytes, macrophages and lymphocytes. This polyfunctional molecule is implicated in interactions with target cells mediating signaling, immunomodulation, migration and attachment [47,48]. In the cardiovascular system, OPN levels markedly augment under pathological conditions [49]. Infiltrating leukocytes are relevant cells expressing this agent in inflammatory heart disorders, yet the

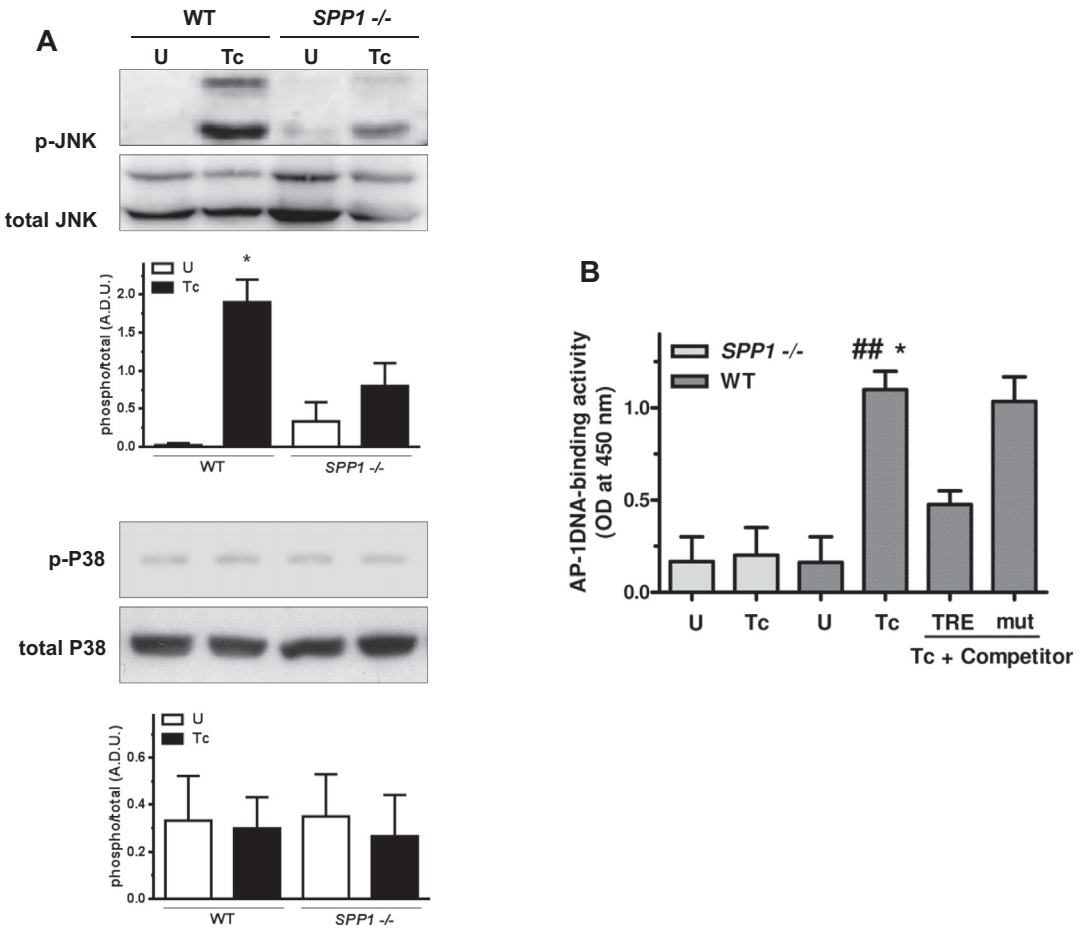

Fig. 4. Involvement of MAPK signaling pathway in osteopontin-dependent cardiopathogenesis in *T. cruzi*-infected mice.
(A) Induction of MAPK signaling pathway. The hearts from infected (Tc, black bars) WT and *spp1* −/− mice were collected at 100 dpi and lysed as described in 'Material and methods'. Cardiac homogenates from uninfected animals (U, white bars) were included as controls. The lysates were analyzed by Western immunoblotting using antibodies to total (p38 and JNK) and phosphorylated (p-p38 and p-JNK) kinases. Band intensity was analyzed using NIH Image J software. A.D.U., arbitrary densitometric units.
(B) ELISA for AP-1 (c-jun) DNA-binding activity. Nuclear extracts from uninfected (U) and infected (Tc, 100 dpi) WT (dark grey bars) and *spp1* −/− (light grey bars) murine hearts (at least eight individual samples from each group collected from three separate experiments) were assayed in triplicate. Activated phospho-c-jun present in infected WT samples recognizes an oligonucleotide containing the consensus binding motif immobilized on the microplate. Specificity of the assay was confirmed by competition of phosphorylated c-jun binding by addition of unbound original TRE *versus* mutant (mut) oligonucleotide. OD, optical density. Data are the means ± SD of three independent experiments. $^{*}P < 0.05$ *versus* Tc + TRE competitor; $^{\#\#}P < 0.01$ *versus* U- and Tc-*spp1* −/− mice.

potential contribution of OPN derived from infected cardiomyocytes should not be underestimated [50,51]. Further, OPN overexpression has been associated with processes of cardiac remodeling in long-term evolution of myocarditis [52]. After 100 days of infection, we observed that *T. cruzi*-harboring mice genetically lacking OPN presented significant reduction of myocardial enlargement, inflammatory infiltration and interstitial fibrosis when compared with infected WT animals. In the *spp1* −/− group, amelioration of inflammation and tissue damage was associated with downregulated *Ccl5* gene and CCL5 protein expression in the infected heart. In fact, OPN has been reported to effectively drive CCL5 production in mesenchymal stromal cells [53]. It may be speculated that OPN acts as an important and specific stimulus for myocardial CCL5 that boosts the migration of inflammatory cells to the heart of *T. cruzi*-infected WT mice. It is noteworthy that upregulated production of myocardial OPN, CCL5 and MMP-2 strongly correlated with parameters of inflammatory damage and adverse modification of cardiac architecture during experimental chronic Chagas myocarditis. Taken together, these data suggest that endogenous OPN is involved in the pathogenesis of *T. cruzi*-elicited cardiomyopathy upon prolonged infection with this protozoan parasite. Alternatively, other important detrimental actions of OPN in the infected host should be considered to analyze the attenuation of cardiac damage linked to global genetic loss of this matricellular component. Myocardial OPN overexpression has been associated with increased myocyte death and organ dysfunction in different models of heart disease [54]. OPN may interact with CD44 receptor favoring apoptosis *via* oxidative stress, mitochondrial death pathways, and BIK/caspase-12 activities [55]. Moreover, OPN could favor myofibroblast differentiation as well as survival, migration and proliferation of cardiac fibroblasts, ultimately promoting interstitial fibrosis [56,57]. Consequently, reduced heart pathology in *T. cruzi*-infected OPN-deficient mice might be further attributable to diminished levels of cardiomyocyte destruction and enhanced myofibroblast/fibroblast activation.

We then explored the cellular and molecular mechanisms underlying OPN-orchestrated cardiopathogenesis during the chronic stage of *T. cruzi* infection. In persistently infected heart displaying exacerbated OPN expression, it is evident that infiltrating $CD8^+$ T cells are one of the principal producers of CCL5 and MMP-2. Both mediators have been tightly linked to pathological inflammation and cardiac fibrosis, crucial factors in determining the severity of Chagas cardiomyopathy. In agreement with our finding, CCL5 has been detected in cardiac tissue from parasite-infected mice in association with $CD8^+$ T cells [58]. Moreover, this cell subset has been identified as the main cellular origin of MMP-2 and MMP-9 in *T. cruzi*-infected patients with heart failure [39]. In our *in vivo* infection experiments, OPN-deficient mice displayed significantly lower levels of MMP-2 protein in the blood and heart, and

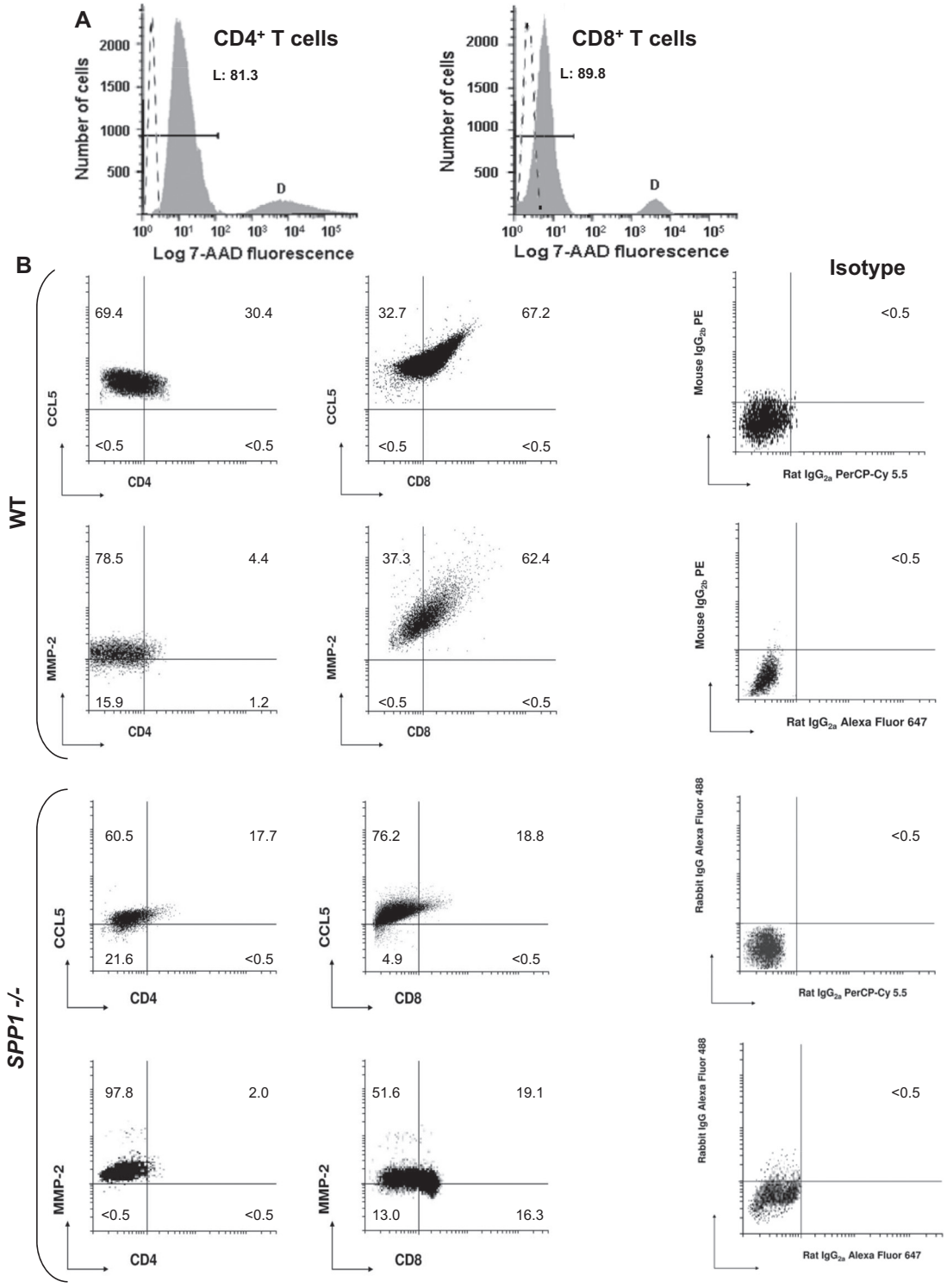

Fig. 5. *Ex vivo* studies of CCL5 and MMP-2 expression in T lymphocytes purified from inflammatory infiltrates present in the hearts of *T. cruzi*-infected (A) WT and (B) *spp1* −/− mice (ten mice per group) after 100 days of infection.

(A) The cells were first stained extracellularly for murine CD4 and CD8 surface markers and gated on viable [7-amino-actinomycin D (7-AAD) negative] lymphocyte subpopulations. Shaded area of histograms represents live -L- and dead -D- cells; dashed curve shows background signal. Percentage lymphocyte viability values are indicated.

(B) $CD4^+$ and $CD8^+$ T cells were stained for intracytoplasmic chemokine/metalloproteinase, as described under 'Material and methods'. The relative number of $CD4^+CCL5^+$, $CD8^+CCL5^+$, $CD4^+MMP\text{-}2^+$, and $CD8^+MMP\text{-}2^+$ cells for each group (at least eight mice per group were analyzed) was determined by flow cytometry (representative plots from three independent experiments are shown). Isotype controls are shown on the right.

less cardiac gelatinase activity, than their WT littermates. Such observations reflect the importance of endogenous OPN for stimulation of MMP-2 production and activity that decisively contributes to the aggravation of chronic *T. cruzi*-elicited cardiomyopathy. MMP-2 activation in the inflamed myocardium, either independently or coupled to other pathogenic mediators like endothelin-1, is known to lead to adverse ventricular enlargement and systolic dysfunction [27,59]. Several studies have addressed this apparently paradoxical boost in

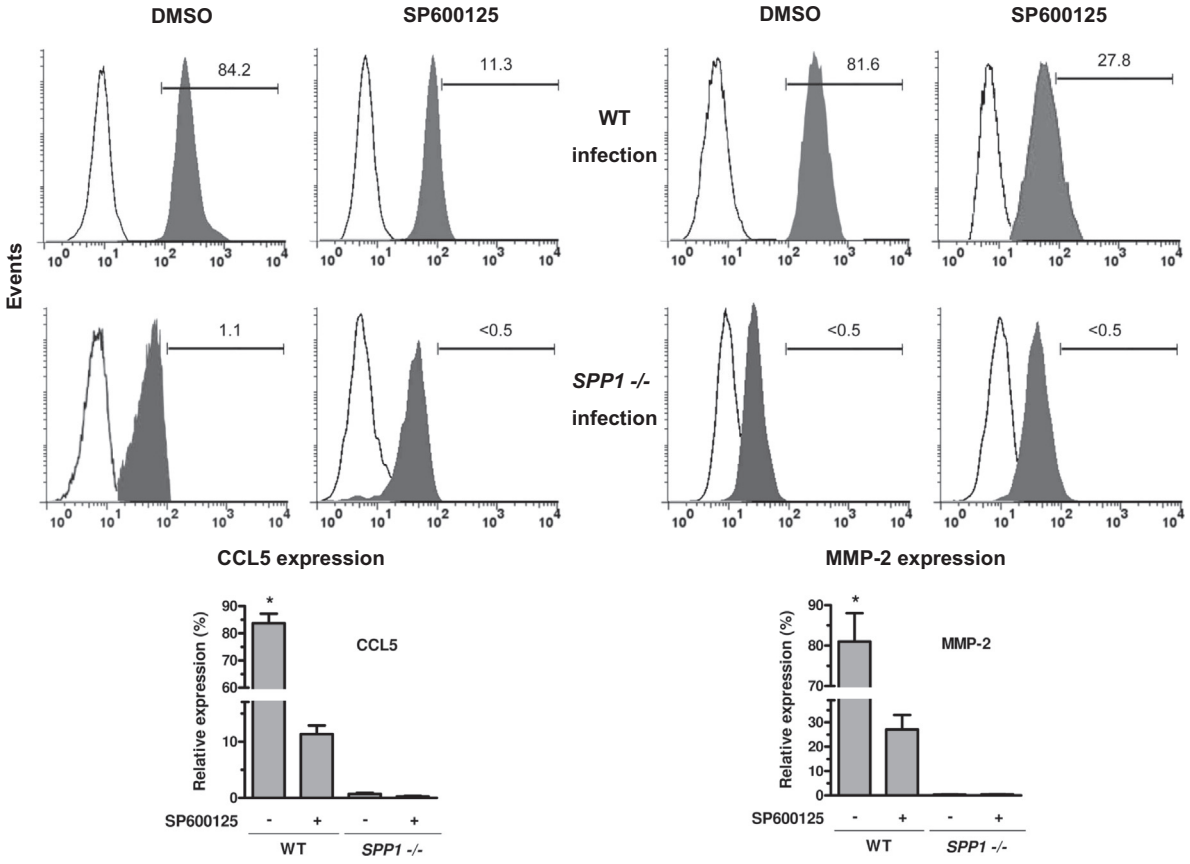

Fig. 6. Modulation of CCL5 and MMP-2 responses through inhibition of JNK MAPK signaling pathway.
$CD8^+$ T cells were purified from inflammatory infiltrates isolated from hearts of *T. cruzi*-infected WT and *spp1* −/− mice on day 100 of infection. Cells were expanded for 72 h in the presence of JNK-specific inhibitor SP600125 at 10 μM as described in 'Material and methods'. Vehicle-treated controls (DMSO) were included for testing. CCL5 and MMP-2 expression was analyzed by flow cytometry. The dark grey-colored histogram represents the expression of each mediator after the addition of inhibitor or vehicle, whereas histogram in white represents the corresponding IgG isotype control. The numbers indicate percentage values of CCL5- and MMP-2-expressing $CD8^+$ T cells. Quantification of the expression of CCL5 and MMP-2 in specimens from infected WT and *spp1* −/− groups is shown. Data are representative of one of three independent experiments, each performed with twenty mice per group. *$P < 0.05$ *versus* infected WT cells incubated with the inhibitor.

MMP-2 activity accompanied by increased heart fibrosis [60–62]. Although a definite explanation is still pending, it should be taken into account that MMP-2 seems to have an array of cardiac remodeling-promoting functions. Elevated activity of this metalloproteinase may potentiate continuous influx of inflammatory cells to the infected muscle through activation of cytokines/chemokines or chemoattraction mediated by degradation products of myocardial matrix components, which could facilitate profibrotic changes [63,64].

OPN is known to be involved in tuning of intracellular signaling cascades controlling the production of pro-inflammatory mediators. Previous reports pointed out that OPN stimulation of mesenchymal stromal cells leads to AP-1 c-jun binding to the *Ccl5* promoter [53]. Also, OPN is capable of triggering MMP-2 expression and its activation *via* the SDF-1α/CXCR4 axis and/or the IκBα/IKK/NF-κB pathway [16,65]. Herein, we characterized endogenous OPN as a potent upregulator of JNK MAPK signaling route and DNA-binding activity of c-jun AP-1 transcription factor in *T. cruzi*- infected myocardium. In parallel, our findings unveil a phospho-JNK MAPK-dependent mechanism of CCL5 and MMP-2 synthesis that operates in infiltrating $CD8^+$ T cells isolated from WT, but not OPN-deficient, mice with chronic infection. Thus, it could be speculated that myocardial OPN overexpression makes a critical contribution to JNK induction and subsequent CCL5/MMP-2 production in $CD8^+$ T cells dominating the inflammatory infiltrate in Chagas myocarditis.

In summary, this study provides evidence, for the first time, that endogenous OPN is a key player in the pathogenesis of inflammatory cardiomyopathy caused by persistent *T. cruzi* infection, through the upregulation of myocardial CCL5/MMP-2 expression and activities, leading to pro-inflammatory and pro-hypertrophic events, cardiac remodeling and interstitial fibrosis. The $CD8^+$ T cell compartment within the inflammatory infiltrate most likely constitutes a major source of these cardiopathogenic agents. So far, the development of *T. cruzi*-driven myocarditis represents interplay of many parasite and host factors. A growing body of evidence suggests that the combined effects of infection, inflammatory mediators and regulatory signals on the cardiovascular system influence the evolution of Chagas cardiomyopathy [2,28,66]. Our current results open new perspectives to gain insight into the complex host-parasite interrelationship and reveal potential novel chemotherapeutic targets for modulating the life-threatening progression of Chagas heart disease.

Supplementary data to this article can be found online at https://doi.org/10.1016/j.bbadis.2017.10.006.

Transparency document

The Transparency document associated with this article can be found, in online version.

Acknowledgements

We gratefully acknowledge following funding: M. H. S. is supported by the Iberoamerican Science Consortium (Grant 2013096); R. S. C. is supported by the National Research Council (CONICET), Argentina (Grant 11220120100518). R. S. C. is a member of the Research Career

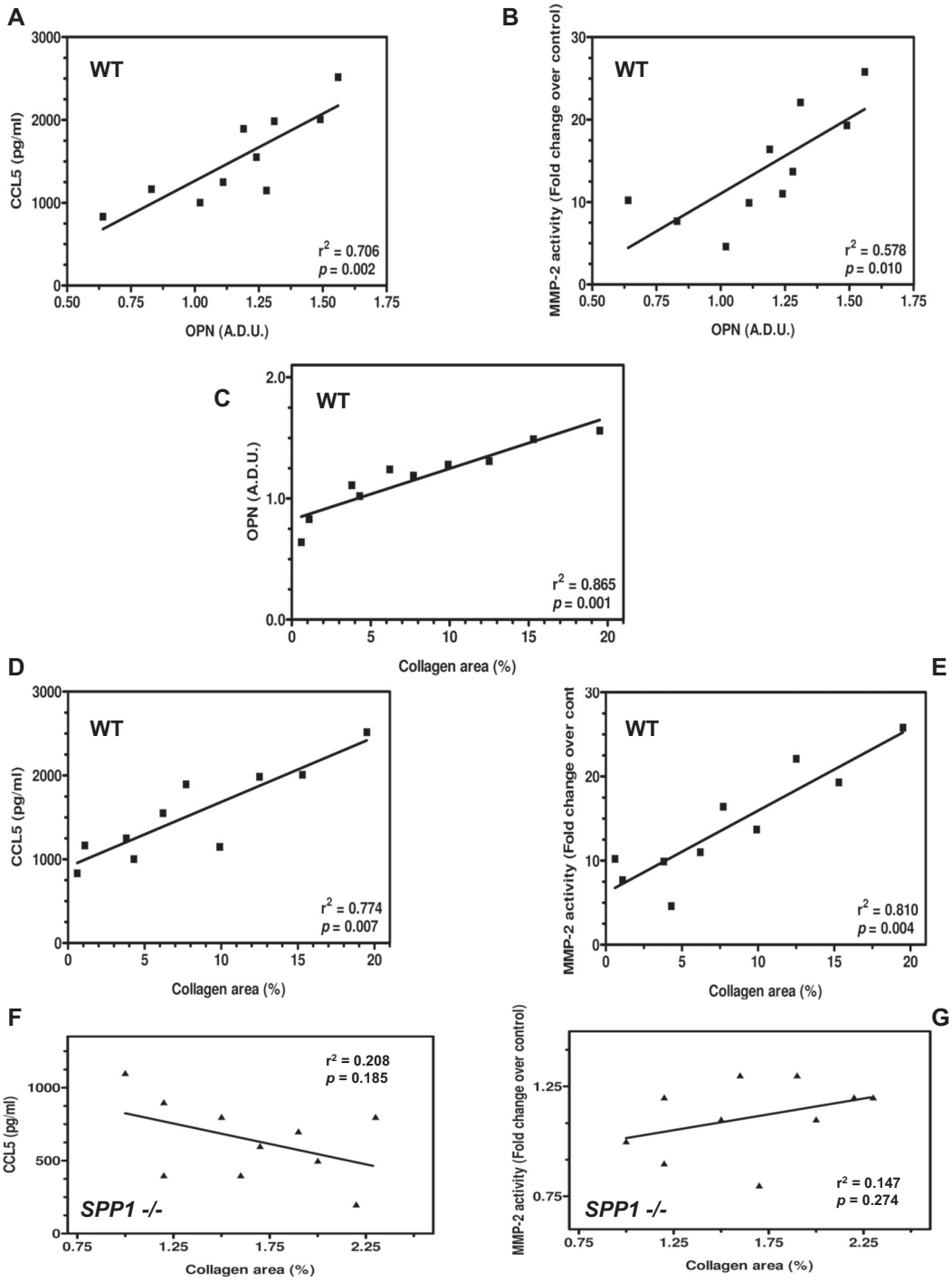

Fig. 7. Correlation analysis of myocardial osteopontin (OPN), CCL5 and MMP-2 with heart fibrosis caused by chronic *T. cruzi* infection.
Plots show correlations between (A) CCL5 levels or (B) MMP-2 activity and OPN expression in cardiac tissues from wild-type (WT) mice upon 100 days of infection. CCL5 concentration was measured by ELISA, relative MMP-2 activity was determined by gelatin zymography and densitometry, and OPN expression was evaluated by immunohistochemistry coupled with image analysis (see Supplemental Fig. 2). A.D.U., arbitrary densitometric units relative to β-actin expression.
Additional plots display correlations between (C) OPN levels, or (D) CCL5 production, or (E) MMP-2 activity, and the percent area of collagen in the infected WT myocardium calculated using data from histopathological studies. Estimated associations of (F) CCL5 levels, or (G) MMP-2 activity, with collagen area (%) in *T. cruzi spp1* −/− hearts are also depicted.
The Spearman correlation coefficient was used for analysis. Significant differences (*P* value) are indicated in each graph, together with the r^2 value. The filled squares (WT) or triangles (*spp1* −/−) represent the individual samples evaluated. The solid lines represent the linear regression for each association.

Program from CONICET. The funding sources had no role in study design; in the collection, interpretation and analysis of data; in the writing of the report; and in the decision to submit the article for publication. The expert technical assistance of Mercedes Miranda Bianco, Julia Hall and Ramiro Pérez Herrera is also greatly acknowledged.

Disclosure

The authors declare no disclosures, financial or otherwise in relation to this work.

References

[1] A.M.B. Bilate, E. Cunha-Neto, Chagas disease cardiomyopathy: current concepts of an old disease, Rev. Inst. Med. Trop. Sao Paulo 50 (2008) 67–74.

[2] J.D. Maya, M. Orellana, J. Ferreira, U. Kemmerling, R. López-Muñoz, A. Morello, Chagas disease: present status of pathogenic mechanisms and chemotherapy, Biol. Res. 43 (2010) 323–331.

[3] M.D. Higuchi, M.M. Ries, V.D. Aiello, L.A. Benvenutti, P.S. Gutierrez, G. Bellotti, F. Pileggi, Association of an increase in $CD8^+$ T cells with the presence of *Trypanosoma cruzi* antigens in chronic, human, chagasic myocarditis, Am. J. Trop. Med. Hyg. 56 (1997) 485–489.

[4] R.L. Tarleton, Parasite persistence in the aetiology of Chagas disease, Int. J. Parasitol. 31 (2001) 549–553.

[5] A.P. Marino, A. da Silva, P. dos Santos, L.M. Pinto, R.T. Gazzinelli, M.M. Teixeira, J. Lannes-Vieira, Regulated on activation, normal T cell expressed and secreted (RANTES) antagonist (Met-RANTES) controls the early phase of *Trypanosoma cruzi*-elicited myocarditis, Circulation 110 (2004) 1443–1449.

[6] A. Rassi Jr., W.C. Little, S.S. Xavier, S.G. Rassi, A.G. Rassi, G.G. Rassi, A. Hasslocher-Moreno, A.S. Sousa, M.I. Scanavacca, Development and validation of a risk score for predicting mortality in Chagas' heart disease, N. Engl. J. Med. 355 (2006) 799–808.

[7] R.P. Somerville, S.A. Oblander, S.S. Apte, Matrix metalloproteinases: old dogs with new tricks, Genome Biol. 4 (2003) 216.

[8] G.T. Brown, G.I. Murray, Current mechanistic insights into the roles of matrix metalloproteinases in tumour invasion and metastasis, J. Pathol. 237 (2015) 273–281.

[9] A. Tokito, M. Jougasaki, Matrix metalloproteinases in non-neoplastic disorders, Int. J. Mol. Sci. 17 (2016) E1178.

[10] N. Geurts, G. Opdenakker, P.E. Van den Steen, Matrix metalloproteinases as therapeutic targets in protozoan parasitic infections, Pharmacol. Ther. 133 (2012) 257–279.

[11] F.R. Gutierrez, M.M. Lalu, F.S. Mariano, C.M. Milanezi, J. Cena, R.F. Gerlach, J.E. Santos, D. Torres-Dueñas, F.Q. Cunha, R. Schulz, J.S. Silva, Increased activities of cardiac matrix metalloproteinases matrix metalloproteinase (MMP)-2 and MMP-9 are associated with mortality during the acute phase of experimental *Trypanosoma cruzi* infection, J Infect Dis 197 (2008) 1468–1476.

[12] F. Penas, G.A. Mirkin, E. Hovsepian, Á. Cevey, R. Caccuri, M.E. Sales, N.B. Goren, PPARγ ligand treatment inhibits cardiac inflammatory mediators induced by infection with different lethality strains of *Trypanosoma cruzi*, Biochim. Biophys. Acta 1832 (2013) 239–248.

[13] N.L. Bautista-López, C.A. Morillo, P. López-Jaramillo, R. Quiroz, C. Luengas, S.Y. Silva, J. Galipeau, M.M. Lalu, R. Schulz, Matrix metalloproteinases 2 and 9 as diagnostic markers in the progression to Chagas cardiomyopathy, Am. Heart J. 165 (2013) 558–566.

[14] E.H. Clark, M.A. Marks, R.H. Gilman, A.B. Fernandez, T.C. Crawford, A.M. Samuels, A.I. Hidron, G. Galdos-Cardenas, G.S. Menacho-Mendez, R.W. Bozo-Gutierrez, D.L. Martin, C. Bern, Circulating serum markers and QRS scar score in Chagas cardiomyopathy, Am. J. Trop. Med. Hyg. 92 (2015) 39–44.

[15] J.E. Sherbuk, E.E. Okamoto, M.A. Marks, E. Fortuny, E.H. Clark, G. Galdos-Cardenas, A. Vasquez-Villar, A.B. Fernandez, T.C. Crawford, R.Q. Do, J.L. Flores-Franco, R. Colanzi, R.H. Gilman, C. Bern, Biomarkers and mortality in severe Chagas cardiomyopathy, Glob. Heart 10 (2015) 173–180.

[16] R. Zhang, X. Pan, Z. Huang, G.F. Weber, G. Zhang, Osteopontin enhances the expression and activity of MMP-2 via the SDF-1/CXCR4 axis in hepatocellular carcinoma cell lines, PLoS One 6 (2011) e23831.

[17] M.H. Santamaría, R.S. Corral, Osteopontin-dependent regulation of Th1 and Th17 cytokine responses in *Trypanosoma cruzi*-infected C57BL/6 mice, Cytokine 61 (2013) 491–498.

[18] S. Mukherjee, T.J. Belbin, D.C. Spray, D.A. Iacobas, L.M. Weiss, R.N. Kitsis, M. Wittner, L.A. Jelicks, P.E. Scherer, A. Ding, H.B. Tanowitz, Microarray analysis of changes in gene expression in a murine model of chronic chagasic cardiomyopathy, Parasitol. Res. 91 (2003) 187–196.

[19] S. Caldas, I.S. Caldas, L.D.F. Diniz, W.G. Lima, R.D. Oliveira, A.B. Cecílio, I. Ribeiro, A. Talvani, M.T. Bahia, Real-time PCR strategy for parasite quantification in blood and tissue samples of experimental *Trypanosoma cruzi* infection, Acta Trop. 123 (2012) 170–177.

[20] D.J. Donnelly, J.C. Gensel, D.P. Ankeny, N. Van Rooijen, P.G. Popovich, An efficient and reproducible method for quantifying macrophages in different experimental models of central nervous system pathology, J. Neurosci. Methods 181 (2009) 36–44.

[21] J.M. Streicher, K. Kamei, T. Ishikawa, H. Herschman, Y. Wang, Compensatory hypertrophy induced by ventricular cardiomyocyte specific COX-2 expression in mice, J. Mol. Cell. Cardiol. 49 (2010) 88–94.

[22] J.T. Liou, D.C. Sum, F.C. Liu, C.C. Mao, Y.S. Lai, Y.J. Day, Spatial and temporal analysis of nociception-related spinal cord matrix metalloproteinase expression in a murine neuropathic pain model, J. Chin. Med. Assoc. 76 (2013) 201–210.

[23] J. Vogt, C.D. Alba Soto, M.P. Mincz, G.A. Mirkin, Impaired *Trypanosoma cruzi*-specific IFN-gamma secretion by T cells bearing the BV9 T-cell receptor is associated with local IL-10 production in non-lymphoid tissues of chronically infected mice, Microbes Infect. 10 (2008) 781–790.

[24] Y.C. Lo, M.A. Edidin, J.D. Powell, Selective activation of antigen-experienced T cells by anti-CD3 constrained on nanoparticles, J. Immunol. 191 (2013) 5107–5114.

[25] K.H. Sonoda, Y. Sasa, H. Qiao, C. Tsutsumi, T. Hisatomi, S. Komiyama, T. Kubota, T. Sakamoto, Y. Kawano, T. Ishibashi, Immunoregulatory role of ocular macrophages: the macrophages produce RANTES to suppress experimental autoimmune uveitis, J. Immunol. 171 (2003) 2652–2659.

[26] M.S. Kim, T. Takahashi, J.Y. Lee, G.W. Hwang, A. Naganuma, Global chemokine expression in methylmercury-treated mice: methylmercury induces brain-specific expression of CCL3 and CCL4, J. Toxicol. Sci. 38 (2013) 925–929.

[27] E. Roffê, F. Oliveira, A.L. Souza, V. Pinho, D.G. Souza, P.R. Souza, R.C. Russo, H.C. Santiago, A.J. Romanha, H.B. Tanowitz, J.G. Valenzuela, M.M. Teixeira, Role of CCL3/MIP-1alpha and CCL5/RANTES during acute *Trypanosoma cruzi* infection in rats, Microbes Infect. 12 (2010) 669–676.

[28] S. Chaneva, G. Schneider, D. Siegmund, H. Wajant, J. Mages, G. Häcker, Enhanced basal AP-1 activity and de-regulation of numerous genes in T cells transgenic for a dominant interfering mutant of FADD/MORT1, Eur. J. Immunol. 34 (2004) 3006–3015.

[29] H.B. Tanowitz, H. Huang, L.A. Jelicks, M. Chandra, M.L. Loredo, L.M. Weiss, S.M. Factor, V. Shtutin, S. Mukherjee, R.N. Kitsis, G.J. Christ, M. Wittner, J. Shirani, Y.Y. Kisanuki, M. Yanagisawa, Role of endothelin 1 in the pathogenesis of chronic chagasic heart disease, Infect. Immun. 73 (2005) 2496–2503.

[30] M.R. Bergman, J.R. Teerlink, R. Mahimkar, L. Li, B.Q. Zhu, A. Nguyen, S. Dahi, J.S. Karliner, D.H. Lovett, Cardiac matrix metalloproteinase-2 expression independently induces marked ventricular remodeling and systolic dysfunction, Am. J. Phys. 292 (2007) H1847–H1860.

[31] Y. Wei, C. Cui, M. Lainscak, X. Zhang, J. Li, J. Huang, H. Zhang, Z. Zheng, S. Hu, Type-specific dysregulation of matrix metalloproteinases and their tissue inhibitors in end-stage heart failure patients: relationship between MMP-10 and LV remodelling, J. Cell. Mol. Med. 15 (2011) 773–782.

[32] A. Talvani, C.S. Ribeiro, J.C.S. Aliberti, V. Michailowsky, P.V.A. Santos, S.M.F. Murta, A.J. Romanha, I.C. Almeida, J. Farber, J. Lannes-Vieira, J.S. Silva, R.T. Gazzinelli, Kinetics of cytokine gene expression in experimental chagasic cardiomyopathy: tissue parasitism and endogenous IFN-γ as important determinants of chemokine mRNA expression during infection with *Trypanosoma cruzi*, Microbes Infect. 2 (2000) 851–856.

[33] P. Augustin, G. Alsalih, Y. Launey, S. Delbosc, L. Louedec, V. Ollivier, F. Chau, P. Montravers, X. Duval, J.B. Michel, O. Meilhac, Predominant role of host proteases in myocardial damage associated with infectious endocarditis induced by *Enterococcus faecalis* in a rat model, Infect. Immun. 81 (2013) 1721–1729.

[34] Y. Xie, M. Li, X. Wang, X. Zhang, T. Peng, Y. Yang, Y. Zou, J. Ge, H. Chen, R. Chen, In vivo delivery of adenoviral vector containing interleukin-17 receptor A reduces cardiac remodeling and improves myocardial function in viral myocarditis leading to dilated cardiomyopathy, PLoS One 8 (2013) e72158.

[35] H.Y. Pan, H.M. Sun, L.J. Xue, M. Pan, Y.P. Wang, H. Kido, J.H. Zhu, Ectopic trypsin in the myocardium promotes dilated cardiomyopathy after influenza A virus infection, Am. J. Physiol. Heart Circ. Physiol. 307 (2014) H922–H932.

[36] A.V. Ovechkin, N. Tyagi, W.E. Rodriguez, M.R. Hayden, K.S. Moshal, S.C. Tyagi, Role of matrix metalloproteinase-9 in endothelial apoptosis in chronic heart failure in mice, J. Appl. Physiol. 99 (2005) 2398–2405.

[37] V. Polyakova, S. Hein, S. Kostin, T. Ziegelhoeffer, J. Schaper, Matrix metalloproteinases and their tissue inhibitors in pressure-overloaded human myocardium during heart failure progression, J. Am. Coll. Cardiol. 44 (2004) 1609–1618.

[38] D. Bironaite, D. Daunoravicius, J. Bogomolovas, S. Cibiras, D. Vitkus, E. Zurauskas, I. Zasytyte, K. Rucinskas, S. Labeit, A. Venalis, V. Grabauskiene, Molecular mechanisms behind progressing chronic inflammatory dilated cardiomyopathy, BMC Cardiovasc. Disord. 15 (2015) 26.

[39] R.C. Fares, JdeA Gomes, L.R. Garzoni, M.C. Waghabi, R.M. Saraiva, N.I. Medeiros, R. Oliveira-Prado, L.H. Sangenis, M.daC Chambela, F.F. de Araújo, A. Teixeira-Carvalho, M.P. Damásio, V.A. Valente, K.S. Ferreira, G.R. Sousa, M.O. Rocha, R. Correa-Oliveira, Matrix metalloproteinases 2 and 9 are differentially expressed in patients with indeterminate and cardiac clinical forms of Chagas disease, Infect. Immun. 81 (2013) 3600–3608.

[40] M. Garcia-Saldivia, G. Lopez-Mendez, L. Berrueta, S. Salmen, J.H. Donis, D.F. Davila, Left ventricular geometry and matrix metalloproteinases 2 and 9 in chronic Chagas heart disease, Int. J. Cardiol. 176 (2014) 565–566.

[41] M. Garcia-Saldivia, G. Lopez-Mendez, L. Berrueta, S. Salmen, J.H. Donis, D.F. Davila, Metalloproteinases 2 and 9 in different stages of chronic Chagas disease, Int. J. Cardiol. 179 (2015) 79–81.

[42] N.I. Medeiros, R.C. Fares, E.P. Franco, G.R. Sousa, R.T. Mattos, A.T. Chaves, M.D. Nunes, W.O. Dutra, R. Correa-Oliveira, M.O. Rocha, J.A. Gomes, Differential expression of matrix metalloproteinases 2, 9 and cytokines by neutrophils and monocytes in the clinical forms of Chagas disease, PLoS Negl. Trop. Dis. 11 (2017) e0005284.

[43] E.E. Okamoto, J.E. Sherbuk, E.H. Clark, M.A. Marks, O. Gandarilla, G. Galdos-Cardenas, A. Vasquez-Villar, J. Choi, T.C. Crawford, R.Q. Do, A.B. Fernandez, R. Colanzi, J.L. Flores-Franco, R.H. Gilman, C. Bern, Chagas Disease Working Group in Bolivia and Peru, Biomarkers in *Trypanosoma cruzi*-infected and uninfected individuals with varying severity of cardiomyopathy in Santa Cruz, Bolivia, PLoS Negl. Trop. Dis. 8 (2014) e3227.

[44] L.A. Jelicks, M. Chandra, J. Shirani, V. Shtutin, B. Tang, G.J. Christ, S.M. Factor, M. Wittner, H. Huang, L.M. Weiss, S. Mukherjee, B. Bouzahzah, S.B. Petkova, M.M. Teixeira, S.A. Douglas, M.L. Loredo, P. D'Orleans-Juste, H.B. Tanowitz, Cardioprotective effects of phosphoramidon on myocardial structure and function in murine Chagas' disease, Int. J. Parasitol. 32 (2002) 1497–1506.

[45] J.L. Durand, B. Tang, D.E. Gutstein, S. Petkova, M.M. Teixeira, H.B. Tanowitz, L.A. Jelicks, Dyskinesis in Chagasic myocardium: centerline analysis of wall motion using cardiac-gated magnetic resonance images of mice, Magn. Reson. Imaging 24 (2006) 1051–1057.

[46] J.L. Durand, S. Mukherjee, F. Commodari, A.P. De Souza, D. Zhao, F.S. Machado, H.B. Tanowitz, L.A. Jelicks, Role of NO synthase in the development of *Trypanosoma cruzi*-induced cardiomyopathy in mice, Am. J. Trop. Med. Hyg. 80 (2009) 782–787.

[47] G. Murugaiyan, A. Mittal, H.L. Weiner, Increased osteopontin expression in

dendritic cells amplifies IL-17 production by CD4$^+$ T cells in experimental autoimmune encephalomyelitis and in multiple sclerosis, J. Immunol. 181 (2008) 7480–7488.
[48] L. Liaw, M.P. Skinner, E.W. Raines, R. Ross, D.A. Cheresh, S.M. Schwartz, C.M. Giachelli, The adhesive and migratory effects of osteopontin are mediated via distinct cell surface integrins, J. Clin. Invest. 95 (1995) 713–724.
[49] B. López, A. González, D. Lindner, D. Westermann, S. Ravassa, J. Beaumont, I. Gallego, A. Zudaire, C. Brugnolaro, R. Querejeta, M. Larman, C. Tschöpe, J. Díez, Osteopontin-mediated myocardial fibrosis in heart failure: a role for lysyl oxidase? Cardiovasc. Res. 99 (2013) 111–120.
[50] M. Singh, A. Ananthula, D.M. Milhorn, G. Krishnaswamy, K. Singh, Osteopontin: a novel inflammatory mediator of cardiovascular disease, Front. Biosci. 12 (2007) 214–221.
[51] M. Satoh, M. Nakamura, T. Akatsu, Y. Shimoda, I. Segawa, K. Hiramori, Myocardial osteopontin expression is associated with collagen fibrillogenesis in human dilated cardiomyopathy, Eur. J. Heart Fail. 7 (2005) 755–762.
[52] K. Graf, Y.S. Do, N. Ashizawa, W.P. Meehan, C.M. Giachelli, C.C. Marboe, E. Fleck, W.A. Hsueh, Myocardial osteopontin expression is associated with left ventricular hypertrophy, Circulation 96 (1997) 3063–3071.
[53] Z. Mi, S.D. Bhattacharya, V.M. Kim, H. Guo, I.J. Talbot, P.C. Kuo, Osteopontin promotes CCL5-mesenchymal stromal cell-mediated breast cancer metastasis, Carcinogenesis 32 (2011) 477–487.
[54] S. Dalal, Q. Zha, C.R. Daniels, R.J. Steagall, W.L. Joyner, A.P. Gadeau, M. Singh, K. Singh, Osteopontin stimulates apoptosis in adult cardiac myocytes via the involvement of CD44 receptors, mitochondrial death pathway, and endoplasmic reticulum stress, Am. J. Physiol. Heart Circ. Physiol. 306 (2014) H1182–H1191.
[55] S. Dalal, Q. Zha, M. Singh, K. Singh, Osteopontin-stimulated apoptosis in cardiac myocytes involves oxidative stress and mitochondrial death pathway: role of a pro-apoptotic protein BIK, Mol. Cell. Biochem. 418 (2016) 1–11.
[56] Y. Lenga, A. Koh, A.S. Perera, C.A. McCulloch, J. Sodek, R. Zohar, Osteopontin expression is required for myofibroblast differentiation, Circ. Res. 102 (2008) 319–327.
[57] J.M. Lorenzen, C. Schauerte, A. Hübner, M. Kölling, F. Martino, K. Scherf, S. Batkai, K. Zimmer, A. Foinquinos, T. Kaucsar, J. Fiedler, R. Kumarswamy, C. Bang, D. Hartmann, S.K. Gupta, J. Kielstein, A. Jungmann, H.A. Katus, F. Weidemann, O.J. Müller, H. Haller, T. Thum, Osteopontin is indispensible for AP1-mediated angiotensin II-related miR-21 transcription during cardiac fibrosis, Eur. Heart J. 36 (2015) 2184–2196.
[58] F.S. Machado, N.S. Koyama, V. Carregaro, B.R. Ferreira, C.M. Milanezi, M.M. Teixeira, M.A. Rossi, J.S. Silva, CCR5 plays a critical role in the development of myocarditis and host protection in mice infected with *Trypanosoma cruzi*, J Infect Dis 191 (2005) 627–636.
[59] D.B. Murray, J.D. Gardner, G.L. Brower, J.S. Janicki, Endothelin-1 mediates cardiac mast cell degranulation, matrix metalloproteinase activation, and myocardial remodeling in rats, Am. J. Physiol. Heart Circ. Physiol. 287 (2004) H2295–H2299.
[60] J.S. Janicki, G.L. Brower, J.D. Gardner, A.L. Chancey, J.A. Stewart Jr., The dynamic interaction between matrix metalloproteinase activity and adverse myocardial remodeling, Heart Fail. Rev. 9 (2004) 33–42.
[61] A.N. Panek, M. Bader, Matrix reloaded: the matrix metalloproteinase paradox, Hypertension 47 (2006) 640–641.
[62] N.T. Le, M. Xue, L.A. Castelnoble, C.J. Jackson, The dual personalities of matrix metalloproteinases in inflammation, Front. Biosci. 12 (2007) 1475–1487.
[63] U. Schönbeck, F. Mach, P. Libby, Generation of biologically active IL-1β by matrix metalloproteinases: a novel caspase-1-independent pathway of IL-1β processing, J. Immunol. 161 (1998) 3340–3346.
[64] N.M. Weathington, A.H. van Houwelingen, B.D. Noerager, P.L. Jackson, A.D. Kraneveld, F.S. Galin, G. Folkerts, F.P. Nijkamp, J.E. Blalock, A novel peptide CXCR ligand derived from extracellular matrix degradation during airway inflammation, Nat. Med. 12 (2006) 317–323.
[65] S. Philip, G.C. Kundu, Osteopontin induces nuclear factor kappa B-mediated promatrix metalloproteinase-2 activation through I kappa B alpha/IKK signaling pathways, and curcumin (diferulolylmethane) down-regulates these pathways, J. Biol. Chem. 278 (2003) 14487–14497.
[66] A. Biolo, A.L. Ribeiro, N. Clausell, Chagas cardiomyopathy—where do we stand after a hundred years? Prog. Cardiovasc. Dis. 52 (2010) 300–316.